

Magnetic properties of sediments in cores from the Mandovi estuary, western India: inferences on provenance and pollution

A. Prajith, V. Purnachandra Rao* and Pratima M. Kessarkar

CSIR - National Institute of Oceanography, Dona Paula – 403 004, Goa

Abstract

Magnetic properties of sediments were investigated in 7 gravity cores recovered along a transect of the Mandovi estuary, western India to understand their provenance and pollution. The maximum magnetic susceptibility of sediments was at least 6 times higher in the upper/middle estuary than in lower estuary/bay. The $\chi_{fd}\%$ and $\chi_{ARM}/SIRM$ of sediments indicated coarse, multi-domain and pseudo-single domain magnetic grains, resembling ore material in the upper/middle estuary and coarse stable single domain (SSD) to fine SSD grains in the lower estuary/bay. Mineralogy parameters indicated hematite and goethite-dominated sediments in the upper/middle estuary and magnetite-dominated sediments in the lower estuary/bay. Two sediment types were discernible because of deposition of abundant ore material in the upper/middle estuary and detrital sediment in the lower estuary/bay. The enrichment factor and Index of geo-accumulation of metals indicated significant to strong pollution with respect to Fe and Mn in sediments from the upper/middle estuary.

Corresponding author; e-mail: vp rao@nio.org

Keywords: magnetic properties, ore pollution, estuarine sediments, Mandovi River, western India

Environmental magnetism (EM) has proved to be a powerful diagnostic tool in numerous depositional environments with applications in determining sediment sources (King et al., 1982; Oldfield et al., 1985; Yu and Oldfield, 1989, 1993; Wheeler et al., 1999), assessing post-depositional, diagenetic changes (Karlin and Levi, 1983; Zhang et al., 2001), paleoclimatic (Bloemendal et al., 1992; Vigliotti et al., 1999; Rey et al., 2005; Hayashida et al., 2007) and pollution studies (Bitykova et al., 1999; Petrovsky et al., 2000; Schmidt et al., 2005; Yang et al., 2009; Gudadhe et al., 2012). In this investigation we present the magnetic properties of sediments in cores from the Mandovi estuary, western India (Fig. 1). As the Mandovi is a monsoonal estuary it receives abundant river runoff and sediment discharge only during the wet, monsoon season (June-September) and negligible runoff during dry season (October-May). Estuarine circulation is dominated by tidal and wind-induced currents during dry season and, intrusion of saline water has been reported up to 45 km from the mouth of the estuary (Manoj and Unnikrishnan, 2009). Since 1940, mining for Fe-Mn ores has been an important activity in the drainage basin of the Mandovi River. As fine-grained ore deposits are stored on the shores of the estuary abundant ore material is flushed into estuary during heavy monsoon rains. Ore deposits are also loaded onto barges at several Iron-ore loading dock stations along the upper estuary (see Fig. 1) and transported through the channel of the estuary to the port, where they are loaded onto merchant ships for export. As a consequence one would expect spilling over of ore material from barges into the estuary. The amount of ore material exported is increasing year after year. About 31 million tonnes (mt) of ore deposits were transported through the Mandovi estuary in 2004 (Rangaraj and Raghuram, 2005). The estuarine sedimentation in Mandovi estuary is thus influenced by detrital sediments, ore material and organic sediments. During early diagenesis Fe and Mn minerals get dissolved and reduced forms of these metals are available abundantly in the pore waters and detrimental to the benthic organisms. The purpose of this paper is to report the magnetic properties and Fe and Mn contents of sediments in cores from the Mandovi estuary in order to determine the sources and diagenetic signatures of magnetic minerals in different cores and pollution level of Fe and Mn in the sediments due to ore mining activities.

Seven sediment cores were collected along a 32 km transect of the Mandovi estuary (Fig. 1), using gravity corer and with the help of a scuba diver. The length of recovered sediment varied in each core and it was longer in cores from the upper/middle estuary and shorter in cores from the lower estuary/bay (Table 1). The sediments in the cores were sectioned at 1 cm interval and were oven dried at $<40^{\circ}\text{C}$. For magnetic measurements the dried samples were gently crushed and transferred into tightly packed, plastic bottles. The procedure for magnetic measurements and calculation of environmental magnetic concentration (χ_{lf} , χ_{ARM} and SIRM), grain size ($\chi_{\text{ARM}}/\text{SIRM}$, $\chi_{\text{ARM}}/\chi_{\text{lf}}$, $\text{SIRM}/\chi_{\text{lf}}$)

and mineralogy (S-ratio) parameters given elsewhere (Walden et al., 1999; Kumar et al., 2005) was followed. The range of values of magnetic parameters for all cores is given in Table 1. Figs. 2A-D shows the distribution of magnetic properties of sediments in representative cores. Selected sediment samples were analyzed for mineralogy on a Rigaku X-ray powder diffractometer, using nickel filtered Cu K α radiation (Fig. 3)

The grain size analysis of sediments was carried out by using a laser Malvern Laser Particle size analyzer (Master sizer 2000), after separating the sand fraction. Thereafter the percentages of sand (<2000 μm - >63 μm), silt (<63 μm - >4 μm) and clay (< 4 μm) were calculated in each sample and shown in Figs. 2A-2D. The total carbon content of the sediments was determined by using a NC soil analyzer (FLASH 2000 Organic Elemental Analyzer); Soil NC was used as standard reference material. The total inorganic carbon content was calculated from CaCO₃ content, which was measured using a coulometer (UIC, Inc-CM5130 acidification module). Organic carbon (OC) content was then calculated by subtracting total inorganic carbon from the total carbon in the sediments. The geochemical analysis of metals was carried out on a Perkin Elmer Optical Emission Spectrometer (Optima 7300 DV) and the entire method was reported in Prajith et al. (2015). The reproducibility of the geochemical analyses for metals was better than $\pm 10\%$. Age of the sediments by ²¹⁰Pb excess method was not successful (Prajith et al., 2015). As the CaCO₃ content of the sediments is <2% it is not possible to determine the age of sediments by radiocarbon method. Since the estuarine sediments contain a mixture of different proportions of terrestrial and marine organic matter and also labile and refractory organic matter, the ages based on total organic matter in estuarine sediments have limitations and should be interpreted cautiously. As we have no other option we have determined the total organic carbon (TOC) ages of sediments in cores from the upper estuary, lower estuary and bay, measured by Accelerator Mass Spectrometer (AMS) at NOSAMS facility, Woods Hole Oceanographic Institution, USA. The sediment intervals for which the AMS ages of TOC were obtained are shown in Fig. 2A, Fig. 2C and Fig. 2D. As the $\delta^{13}\text{C}$ of organic carbon of the dated sediments indicate terrestrial organic matter (-27 to -26‰) in the upper estuary and marine organic carbon (-23 to -22‰) in the lower estuary and bay and we believe that the ages are reliable. The ages of sediments from the upper estuary indicate modern sediments (Fig. 2A), whereas those in the lower estuary and bay showed maximum ages of 1588 years A.D. and 539 years A. D., respectively at the bottom portions of the cores (Figs. 2C-D). The age vs. depth plots for the sediments of the lower estuary and bay are given as inserts in Fig. 1.

For convenience of description of results, the magnetic properties of sediments from one representative core in each environment, i. e., upper estuary, middle estuary, lower estuary and Aguada Bay are described here in detail. The sediments exhibit significant variations in color, texture, OC, Fe and Mn content and rock magnetic parameters, both spatially and temporally (Table 1; Fig. 2A-D). The sediments in cores from the upper/middle estuary are reddish brown or, reddish brown to brown in colour (Figs. 2A-B). The sediments in the upper estuary are clayey silts intercalated with sand-dominated sediments, and those in the middle estuary are sandy silts in the lower part and silty sands in the upper parts of the core (Fig. 2A-B). The sediments from the lower estuary were brownish in the upper part and dark brown in the lower part of the core (Fig. 2C). Silty clays intercalated with sand-dominated sediments were characteristic in the upper section of this core. The sediments of the Aguada Bay were brownish in the upper part and greenish in the lower part. Sandy sediments in the lower part of the core were overlain by silty clays at middle part and then by sandy silts in the upper part (Fig. 2D). The OC content varies from 0.4% to 4.5% in different cores and increases towards core top, almost in all the cores.

The magnetic susceptibility (χ_{if}) values of estuarine sediments are usually low ($<50 \times 10^{-8} \text{m}^3 \text{kg}^{-1}$; Booth et al., 2005), but the values up to a maximum of $125 \times 10^{-8} \text{m}^3 \text{kg}^{-1}$ have been reported in tidal flats sediments (Zhang and Yu, 2003). The χ_{if} values reported here are unusually high and ranges from 229 to $2194 \times 10^{-8} \text{m}^3 \text{kg}^{-1}$ with a mean value of $617 \times 10^{-8} \text{m}^3 \text{kg}^{-1}$ in cores from the upper estuary and, from 360 to $1779 \times 10^{-8} \text{m}^3 \text{kg}^{-1}$ with a mean value of $655 \times 10^{-8} \text{m}^3 \text{kg}^{-1}$ in cores from the middle estuary (Table 1). The maximum χ_{if} values in different cores from the upper estuary are 5 to 10 times higher than the minimum χ_{if} values in the same cores. Similarly, the maximum χ_{if} value and Fe content in cores from the upper estuary are ~6 and 3-4 times higher than those from the lower estuary/bay, respectively (Table 1). The χ_{ARM} is sensitive to single domain ferrimagnetic mineral and SIRM is an indicator of ferrimagnetic minerals concentration (Maher, 1988). The χ_{if} values of sediments at several intervals in these cores are comparable with that of ore material and suggest that ore material is directly transported and deposited to this part of the estuary. Very high values of χ_{if} , χ_{ARM} and SIRM in the upper/middle estuary sediments (Table 1) may indicate high proportions of iron ore material. Further, the mean Fe (18-25%) and Mn (0.67-1.15%) of sediments in cores from the upper/middle estuary were 3-5 and 10-12 times, respectively higher than in Post-Archean average Australian Shale (PAAS; 5% and 0.09%, respectively; Table 1) and thus suggesting deposition of ore material rich in Fe and Mn in the upper/middle estuary.

X-ray diffraction studies also indicated higher proportion of iron ore minerals in upper/middle estuary than in lower estuary/Aguada Bay (Fig. 3). The S-ratio of sediments provides a measure of the relative amounts of soft ferrimagnetic (low-coercivity) to hard anti-ferromagnetic (high-coercivity) minerals (Evans and Heller, 2003). It ranges from 44 to 99%, with lowest mean ratios in cores from the upper/middle estuary (73-80%) and highest mean ratios in the lower estuary/bay (90-93%; Table 1). The mean S-ratios of sediments from the upper (73%) and middle estuary (80%) are close to that of ore material (88.7%) and indicate abundant high coercivity minerals, such as hematite or goethite. The IRM acquisition curves of sediments from the upper/middle estuary and ore material are, however, similar, and IRM increases gradually with increasing applied field (see Figs. 4A-B). This indicates the presence of high concentration of hard magnetic (anti-ferromagnetic) minerals. On the other hand, the IRM values are much lower in sediments from the lower estuary/bay than in upper/middle estuary. The IRM acquisition curves indicate IRM reached saturation at $\sim 0.3T$, except in a few samples from the upper portions of the cores (Figs. 4C-D). The IRM saturation at $0.3T$ indicates the presence of soft magnetic (ferrimagnetic) minerals (Walden et al., 1999). Both S-ratios (Table 1) and IRM acquisition curves (Figs. 4C-D) of sediments from the lower estuary/bay indicate magnetite is the dominant mineral. In other words, there is a distinct change in magnetic minerals from hematite and goethite-dominated in the upper/middle estuary to magnetite-dominated in the lower estuary/bay.

The $\chi_{fd}\%$ is an effective measurement for detecting super-paramagnetic (SP) grains, whereas $\chi_{ARM}/SIRM$ ratio is an indicator of domain state of magnetic minerals (Dearing et al., 1997; Walden et al., 1999). The plot of $\chi_{fd}\%$ and $\chi_{ARM}/SIRM$ of sediments of all the cores on the diagram (Fig. 5) of Dearing et al. (1997) indicates that the sediments from the upper/middle estuary contain $<10\%$ SP to $<50\%$ SP grains with abundant coarse, multi-domain (MD) and pseudo-single domain (PSD) grains, and those from the lower estuary/bay contain $<10\%$ SP to $>75\%$ SP grains (Fig. 5). The plot of $\chi_{fd}\%$ and $\chi_{ARM}/SIRM$ ratios of ore material on this diagram (see Fig. 5) suggests that it also contains abundant coarse MD/PSD grains with $<50\%$ SP grains. The $\chi_{ARM}/SIRM$ ratios of sediments from the upper/middle estuary plot on either side of the boundary line separating MD+PSD and coarse stable single domain (SSD) grains. The low $\chi_{ARM}/SIRM$ ratios of sediments from the upper/middle estuary and ore material (Table 1) suggest abundant coarse MD+PSD grains (see Yang et al., 2009). The $\chi_{fd}\%$ values of sediments in the upper/middle estuary (more than 60% of samples) are <4 and reach a maxima of 8 and, those from the lower estuary/bay go up to 10 (Fig. 5). Dearing et al. (1997) and Walden et al. (1999) proposed low χ_{fd} ($<4\%$) indicates high proportions of non-SP grains and ore is the source material for these sediments. The $\chi_{fd}\%$ and $\chi_{ARM}/SIRM$ ratios thus indicate abundant ore material in sediments of the upper/middle estuary.

The Fe of the upper estuary sediments shows weak correlation with χ_{lf} , direct correlation with SIRM/ χ_{lf} and inverse correlation with S-ratio (Figs. 6A-C). This implies that Fe is mainly contributed by anti-ferromagnetic minerals in this part of the estuary. Moreover, high SIRM/ χ_{lf} , low S-ratio and inverse correlation between the two in these sediments (Figs. 2A and 6D) indicate dominance of ore material. Comparable SIRM/ χ_{lf} ratios of upper estuary sediments and ore material (Table 1) argue abundant ore material in the sediments. Walden et al. (1999) and Frank and Nowczyk (2008) proposed high SIRM/ χ_{lf} ratio when associated with low S-ratio indicates the dominance of hematite and goethite.

The increase in OC content coincides with decrease in Fe and Mn towards core top in sediments of the upper estuary (Fig. 2A). On the other hand, the increasing S-ratio towards core top supports increase of fine-grained magnetites and decrease in anti-ferromagnetic minerals (Fig. 2A). These observations suggest that the decrease in Fe and Mn content towards core top may not be due to diagenesis but due to decrease in deposition of ore material and increase in deposition of detrital magnetite transported from land. On the other hand, low magnetic concentration parameters coinciding with high magnetic grain size ratios, high OC and relatively low Fe at lower sections of the core from middle estuary (Fig. 2B) indicate enrichment of fine-grained magnetic minerals either due to authigenic formation of magnetite by early diagenesis or deposition of fine-grained, detrital magnetite during low-energy conditions of the estuary. Similarly, the upper section of the same core exhibits high magnetic concentration parameters coinciding with low magnetic grain size ratios, high Fe and low OC (Fig. 2B) suggesting increase in relatively coarser magnetic particles, most probably due to the deposition of ore material. However, similar mean S-ratio% of both sections (80; Table 1) implies dominant contribution from anti-ferromagnetic minerals compared to the fine-grained, diagenetic or detrital magnetite.

The organic carbon-rich, clayey sediments at upper sections of the core in the lower estuary (Fig. 2C) and middle section of the core in the bay (Fig. 2D) exhibit high χ_{fd} %, χ_{ARM} /SIRM and S-ratio indicating high proportions of SP grains and abundant fine stable single domain (FSSD) grains and authigenic magnetite. Abrajevitch and Kodama (2011) suggested that the bulk of single domain (SD) fraction is biologically produced and is likely to be authigenic. Here ferric iron (Fe^{3+}) may have been reduced to divalent state (Fe^{2+}) during early diagenesis and magnetite could have formed by authigenic and/or biogenic processes. Low sedimentation rates (1 mm/year) at upper sections of the cores in the lower estuary/bay (Fig. 1) may have facilitated the formation of authigenic magnetites. The dark brown, organic carbon-rich (~3%) clayey silts in lower estuary show uniformly low magnetic concentration/grain size ratios and high S-ratios indicating reductive diagenesis in the sediments (Fig. 2C). High concentrations of redox sensitive metals (V/Al, U/Al and Mo/Al) indeed suggest reducing conditions in these sediments (Fig. 7). The oxidative decomposition of organic matter in sediments lead to sulphate

reducing conditions, in which detrital/biogenic magnetites and other iron oxides become progressively reduced or, transformed into pyrites or greigites (see Bloemendal et al., 1992; Kumar et al., 2005; Rao et al., 2010; Roberts, 1995; Liu et al., 2004; Hayashida et al., 2007; Rowan et al., 2009). Greigite is a ferrimagnetic iron sulphide that forms before pyrite. Kao et al. (2004) suggested that the formation of greigite/pyrite may be limited by the rates of supply of decomposable organic matter, dissolved sulfur and reactive iron. As detrital magnetites get dissolved in reducing conditions, high S-ratios (Fig. 2C) may indicate the formation of greigite, which exhibits high S-ratios (Roberts 1995).

Magnetic susceptibility (χ_{lf}) has been used for determining pollution (Bitykova et al., 1999; Petrovsky et al., 2000). Very high χ_{lf} , low $\chi_{ARM}/SIRM$, $\chi_{fd}\%$ and S-ratios indicate abundant anti-ferromagnetic minerals with coarse, MD+PSD grains and high proportions of non-SP grains in sediments of the upper/middle estuary, similar to that of ore material. Further, the mean enrichment factor (mEF) and Index of geo-accumulation (I_{geo}) of metals are the indices to compute the sedimentary metal source contributed by anthropogenic or natural sources. The mEF and I_{geo} values of Fe and Mn (Figs. 8A-B) indicate that the sediments from the upper/middle estuary are in the range 'significant to strong pollution' and those from the lower estuary/bay are in the range 'minimum pollution'. High Fe and Mn contents in the upper/middle estuary are due to ore material transported into the estuary

Magnetic properties, mineralogy, geochemical characteristics and AMS ages of the sediments of the Mandovi estuary indicate (a) high sedimentation rates and ore material-dominated sediments in the upper/middle estuary and, low sedimentation rates and detrital-dominated sediments in the lower estuary/bay. (b) Magnetic minerals are influenced by early diagenesis at high OC intervals in the cores. (c) The Fe and Mn contents of sediments in cores from the upper/middle estuary exhibit significant to strong pollution with respect to these metals. We suggest that the mining and transport of ore through the estuary will further deteriorate the benthic environment and detrimental to the productivity and health of benthic fauna in the estuary.

Acknowledgments: We thank the Director, National Institute of Oceanography for the facilities and encouragement. We thank the anonymous reviewer of our paper for encouraging comments and editorial corrections. Prajith thanks University Grants Commission (UGC) for awarding UGC-NET research fellowship. We thank Mr. Uday Mandrekar for helping us to recover sediment cores by diving and injecting the corer into the sediment. We also thank Dr. C. Prakash Babu and Mr. Girish Prabhu for their help with CNS analyzer and X-ray diffractometer, respectively.

References

- Abrajevitch, A., Kodama, K., 2011. Diagenetic sensitivity of paleoenvironmental proxies, A rock magnetic study of Australian continental margin sediments. *Geochem. Geophys. Geosyst.* 12, 1-18.
- Bitykova, L., Scolger, R., Birke, M., 1999. Magnetic susceptibility as Indicator of Environmental Pollution of Soils in Tallinn. *Phys. and Chem. Earth* 24, 829-835.
- Bloemendal, J., King J.W., Hall, F.R., Doh, S.J., 1992. Rock magnetism of Late Neogene and Pleistocene deep-sea sediments: relationship to sediment source, diagenetic processes and sediment lithology. *J. Geophys. Res.* 97, 4361-4375.
- Booth, C.A., Walden, J., Neal, A., Smith, J.P., 2005. Use of mineral magnetic concentration data as a particle size proxy: A case study using marine, estuarine and fluvial sediments in the Carmarthen Bay area, South Wales, U. K. *Sci. Total Environ.* 347, 241-253.
- Canfield, D.E., 1989. Reactive iron in Marine sediments. *Geochim. Cosmochim. Acta.* 53, 619-632.
- Dearing, J.A., Bird, P.M., Dann, R.J.L., Bejamin, S.F., 1997. Secondary ferromagnetic minerals in Welsh soils: a comparison of mineral magnetic detection methods and implications for mineral formation. *Geophys. J. Int.* 130, 727-736.
- Evans, M.E., Heller, F., 2003. *Environmental Magnetism, Principles and Applications of Enviromagnetics.* Academic Press, pp. 299.
- Forster, U., Ahlf, W., Calmano, W., Kersten, M., 1990. Sediment criteria development-contributions from environmental geochemistry to water quality management. In: Heling D, Rothe P, Forstner U, Stoffers P (eds) *Sediments and environmental geochemistry: selected aspects and case histories.* Springer, Berlin, pp 311–338.
- Frank, U., Nowaczyk, N.R., 2008. Mineral magnetic properties of artificial samples systematically mixed from hematite and magnetite. *Geophys. J. Int.* 175, 449-461.
- Gudadhe, S.S., Sangode S.J., Patil S.K., Chate D.M., Meshram D.C., Badekar A.G., 2012. Pre- and post- monsoon variations in the magnetic susceptibilities of soils of Mumbai metropolitan region: implications to surface redistribution of urban soils loaded with anthropogenic particulates. *Environ. Earth Sci.* 67, 813-831.
- Hayashida, A., Hattori, S., Oda, H., 2007. Diagenetic modification of magnetic properties observed in a piston core (MD01-2407) from the Oki Ridge, Japan. *Palaeogeogr. Palaeoclimatol. Palaeoecol.* 247, 65-74.
- Kao, S.J., Horng, C.S., Roberts, A.P., Liu, K.K., 2004. Carbon–sulfur–iron relationships in sedimentary rocks from southwestern Taiwan: Influence of geochemical environment on greigite and pyrrhotite formation. *Chem. Geol.* 203, 153-168.
- Karlin, R., Levi, S., 1983. Diagenesis of magnetic minerals in the recent hemipelagic sediments. *Nature* 303, 327-330.

- King, J., Banerjee, S.K., Marvin, J., Ozdemir, O., 1982. A comparison of different magnetic methods for determining the relative grain size of magnetite in natural materials: some results from lake sediments. *Earth. Planet. Sc. Lett.* 59, 404-419.
- Kumar, A.A., Rao V.P., Patil, S.K., Kessarkar, P.M., Thamban, M., 2005. Rock magnetic records of the sediments of the eastern Arabian Sea: evidence for late Quaternary climatic change. *Mar. Geol.* 220, 59–82.
- Lee, D.S., Garland, J.A., Fox, A.A., 1994. Atmospheric concentrations of trace elements in urban areas of the United Kingdom. *Atmos. Environ.* 16, 2691- 2713.
- Liu, J., Zhu, R., Roberts, A.P., Li, S., Chang, J.H., 2004. High-resolution analysis of early diagenetic effects on magnetic minerals in post-middle-Holocene continental shelf sediments from the Korea Strait. *J. Geophys. Res.* 109 (B03103), 1–15.
- Maher, B.A., 1988. Magnetic properties of some synthetic sub-micron magnetites. *Geophys. J.* 94, 83-96.
- Manoj, N.T., Unnikrishnan, A.S., 2009. Tidal circulation and salinity distribution in the Mandovi and Zuary estuaries: a case study. *J. Waterw. Port. C-ASCE* 135, 278-287.
- Oldfield F., Maher, B.A., Donoghue, J., Pierce J., 1985. Particle size mineral magnetic source sediment linkages in the Rhodes River Catchment, Maryland, USA. *J. Geol.* 142, 1035-1046.
- Petrovsky, E., Kapica, A., Jordanova, N., Knab, M., Hoffmann, V., 2000. Low-field magnetic susceptibility: A proxy method of estimating increased pollution of different environmental systems. *Environ. Geol.* 39, 3-4.
- Prajith, A., Rao, V.P., Kessarkar, P.M., 2015. Controls on the distribution and fractionation of yttrium and rare earth elements in core sediments from the Mandovi estuary, western India. *Cont. Shelf Res.* 92, 59-71.
- Rangaraj, N., Raghuram, G. 2005. Viability of inland water transport in India—a report. Presented at the Workshop 'Strengthening Policy Reforms for Transport Development in India', sponsored by Asian Development Bank and Department of Economic Affairs, Delhi, 35 pp.
- Rao, V.P., Kessarkar, P.M., Thamban, M., Patil, S.K., 2010. Paleoclimatic and diagenetic history of the Late Quaternary sediments in a core from the Southeastern Arabian sea: Geochemical and magnetic signals. *J. Oceanogr.* 66, 133-146.
- Rey, D., Mohamed, K.J., Bernabeu, A., Rubio, B., Vilas, F., 2005. Early diagenesis of magnetic minerals in marine transitional environments: geochemical signatures of hydrodynamic forcing. *Mar. Geol.* 215, 215-236.
- Roberts, A.P., 1995. Magnetic properties of sedimentary greigite. *Earth and Planet. Sci. Lett.* 134, 227-236.
- Rowan, C.J., Roberts, A.P., Broadbent, T., 2009. Reductive diagenesis, magnetic dissolution, greigite growth and paleomagnetic smoothing marine sediments: A new view. *Earth Planet. Sci. Lett.* 277, 223-235.

- Schmidt, A., Yarnold, R., Hill, M., Ashmore, M., 2005. Magnetic susceptibility as proxy for heavy metal pollution: a case study. *J. Geochem. Explor.* 85, 109-117.
- Sutherland, R. A., 2000. Bed sediment-associated trace metals in an urban stream, Oahu Hawaii. *Environ. Geol.* 39 (6), 611-627.
- Vigliotti, L., Capotondi, L., Toril, M., 1999. Magnetic properties of sediments deposited in suboxic-anoxic environments: relationships with biological and geochemical proxies. *Paleomagnetism and Diagenesis in sediments*, *Geol. Soc. London Spec. Publ.* 151, 71-83.
- Walden, J., Oldfield, F., Smith, J., 1999. *Environmental magnetism. A Practical Guide.* No.6. Quaternary Research Association, London, pp. 243.
- Wheeler, A.J., Frank Oldfield, Julian, D. O., 1999. Depositional and post-depositional controls on magnetic signals from saltmarshes on the north-west coast of Ireland. *Sedimentology* 46, 545-558.
- Yang, T., Liu, Q., Zeng, Q., Chan L., 2009. Environmental magnetic responses of urbanization processes: evidences from lake sediments in East Lake, Wuhan, China. *Geophys. J. Int.* 179, 873-886.
- Yu, L., Oldfield F., 1989. A multivariate mixing model for identifying sediment source from magnetic measurements. *Quat. Res.* 32, 168-181.
- Yu, L., Oldfield, F., 1993. Quantitative sediment ascription using magnetic measurements in reservoir-catchment system near Nijar, S. E Spain. *Earth Surf. Proc. Land.* 18, 441-454.
- Zhang, W., Yu L., Hutchinson, S.M., 2001. Diagenesis of magnetic minerals in the intertidal sediments of the Yangtze Estuary, China, and its environmental significance. *Sci. Total Environ.* 266, 169-175.
- Zhang, W., Yu, L., 2003. Magnetic properties of tidal flat sediments of the Yangtze Estuary and its relationship with particle size. *Sci. China Ser. D* 46, 954-066.

Figure captions

Fig. 1. Location of sediment cores in the Mandovi estuary. Locations of iron ore loading docks, iron ore plant and ship building plant along the shore of the estuary are also shown. Number in parenthesis (next to the name of the sampling station) indicates distance of the core from mouth of the estuary. The plots of age (calibrated AMS age) vs. depth in the core for the cores from the lower estuary and bay are also shown as insert figures at respective locations.

Figs. 2A-D. Down-core variations of sand, silt and clay content, organic carbon (OC), Fe and Mn content and magnetic parameters of the sediments in cores from the upper estuary (A), middle estuary (B), lower estuary (C) and Aguada Bay (D)

Fig. 3 X-ray diffractograms of ore material and core top sediments from representative cores. Q-quartz, H-hametite, M-magnetite, G-goethite, F-feldspar.

Fig. 4. A-D. Selected isothermal remanent magnetization (IRM) acquisition curves of the sediments in different cores. IRM acquisition curve of ore material is also shown in Fig. 4A.

Fig. 5. The plot of $\chi_{fd}\%$ versus $\chi_{ARM}/SIRM$ ratio of sediments from representative cores. Coarse SSD – coarse stable single domain grains; Fine SSD – fine stable single domain grains; SP- Super-paramagnetic grains. Iron ore values are also plotted.

Fig. 6. Correlations of Fe with χ_{if} (A), $SIRM/\chi_{if}$ (B) and S-ratio (C) and S-ratio vs. $SIRM/\chi_{if}$ (D) of sediments in different cores from the Mandovi estuary.

Fig. 7. Down-core variations of redox-sensitive elements (Al-normalized ratios) and OC in sediments from the lower estuary. Dashed vertical line indicates the element/Al ratio of Post-Archaen average Australian Shale (PAAS).

Fig. 8. (A) Mean enrichment factors (mEF) and (B) Index of geo-accumulation (I_{geo}) of Fe and Mn in sediment cores. The defined categories of degree of pollution based on the EF of metals following Lee et al. (1994) and Sutherland (2000) and, I_{geo} values following Forstner et al. (1990) are also shown in the figures.

Table caption

Table 1. Range and mean values of magnetic parameters, Fe and Mn concentrations in sediment cores from the Mandovi estuary.

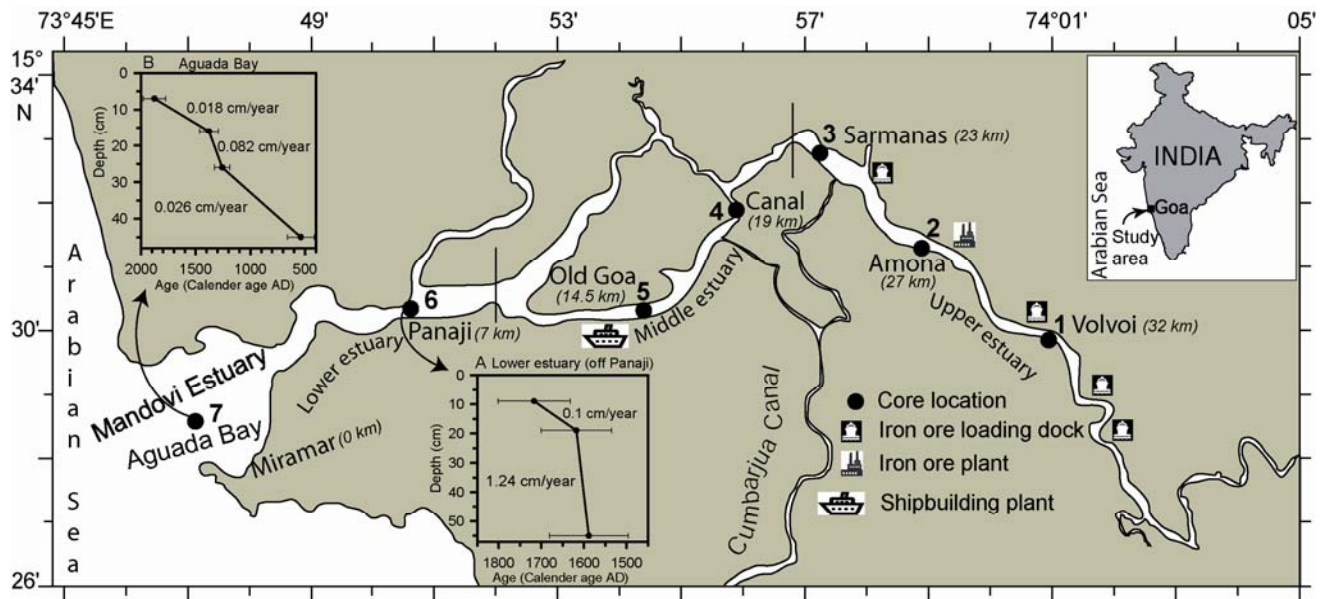


Figure 1

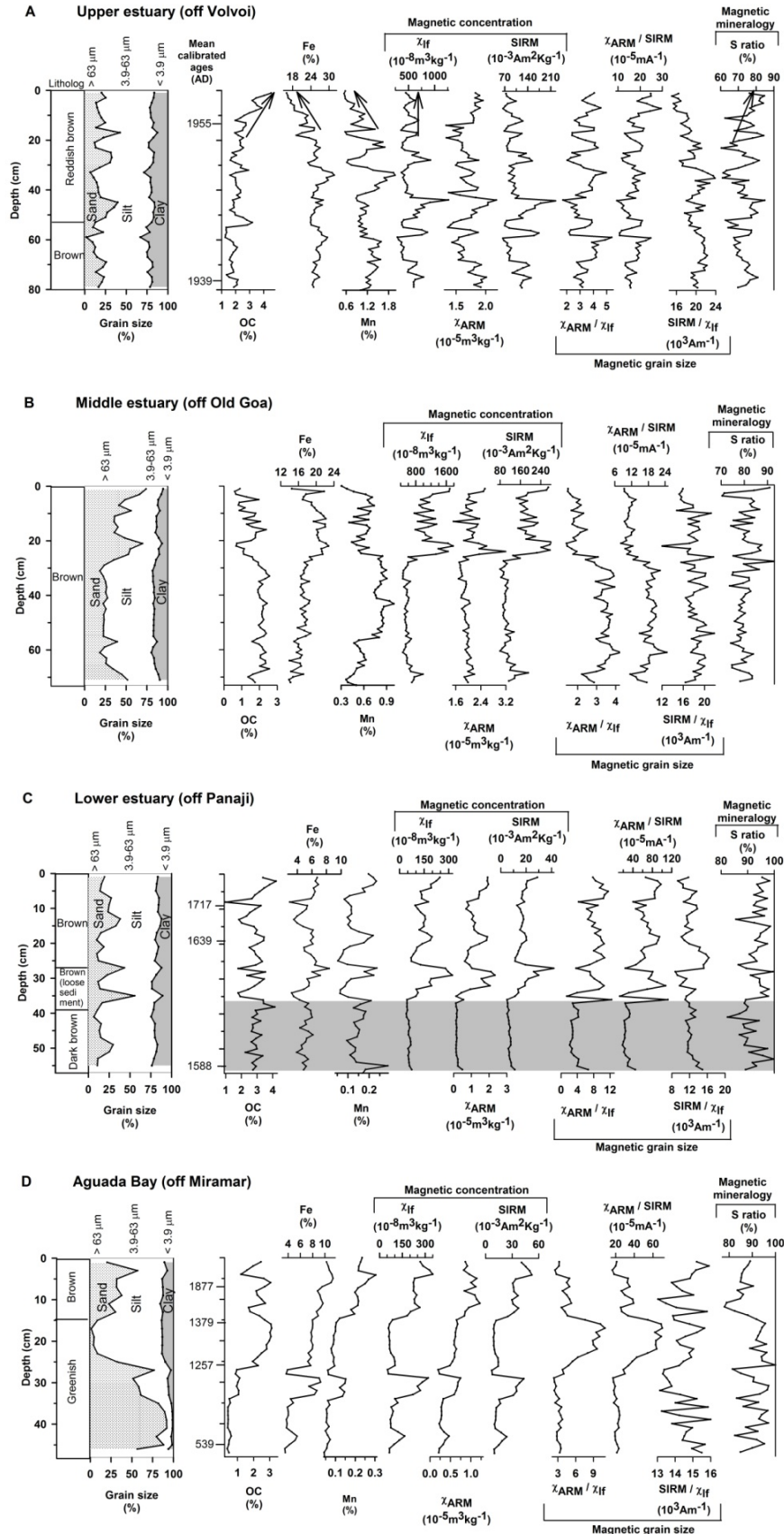


Figure 2

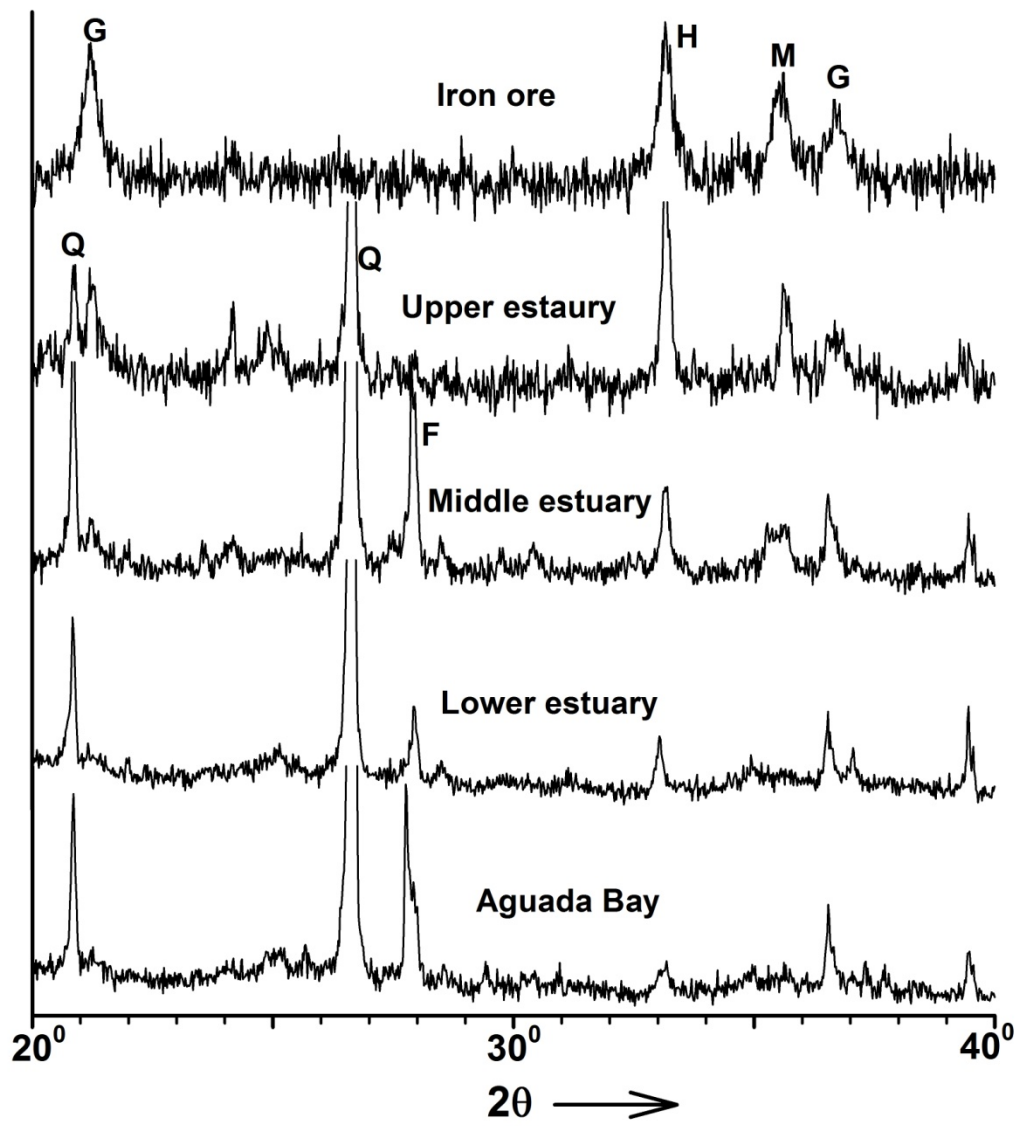


Figure 3

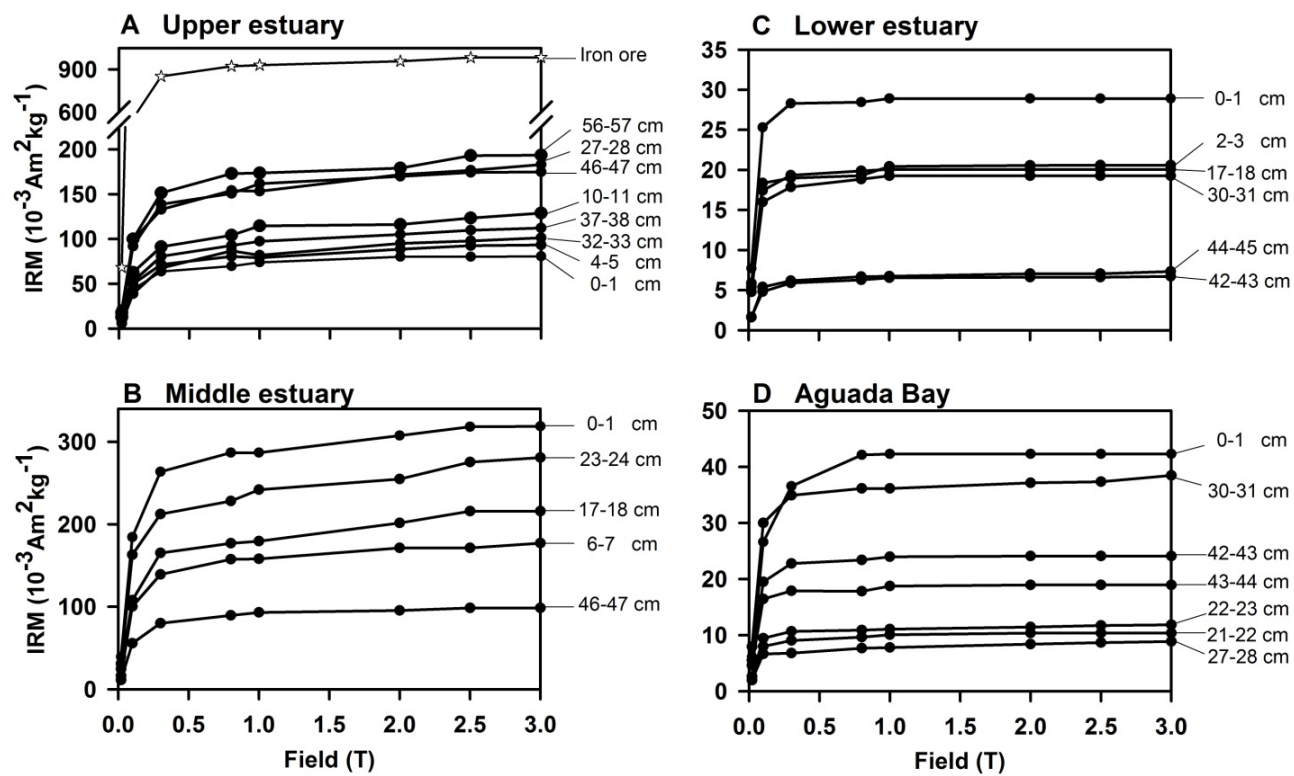


Figure 4

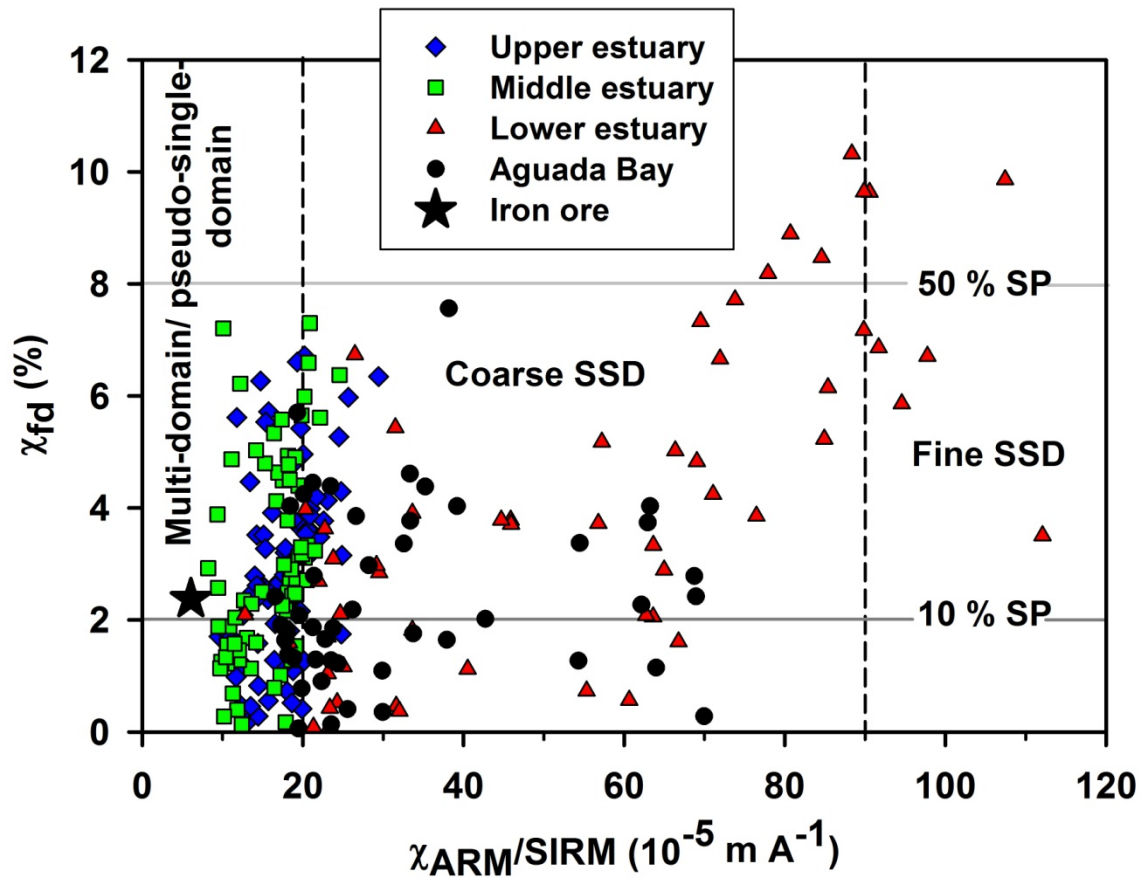


Figure 5

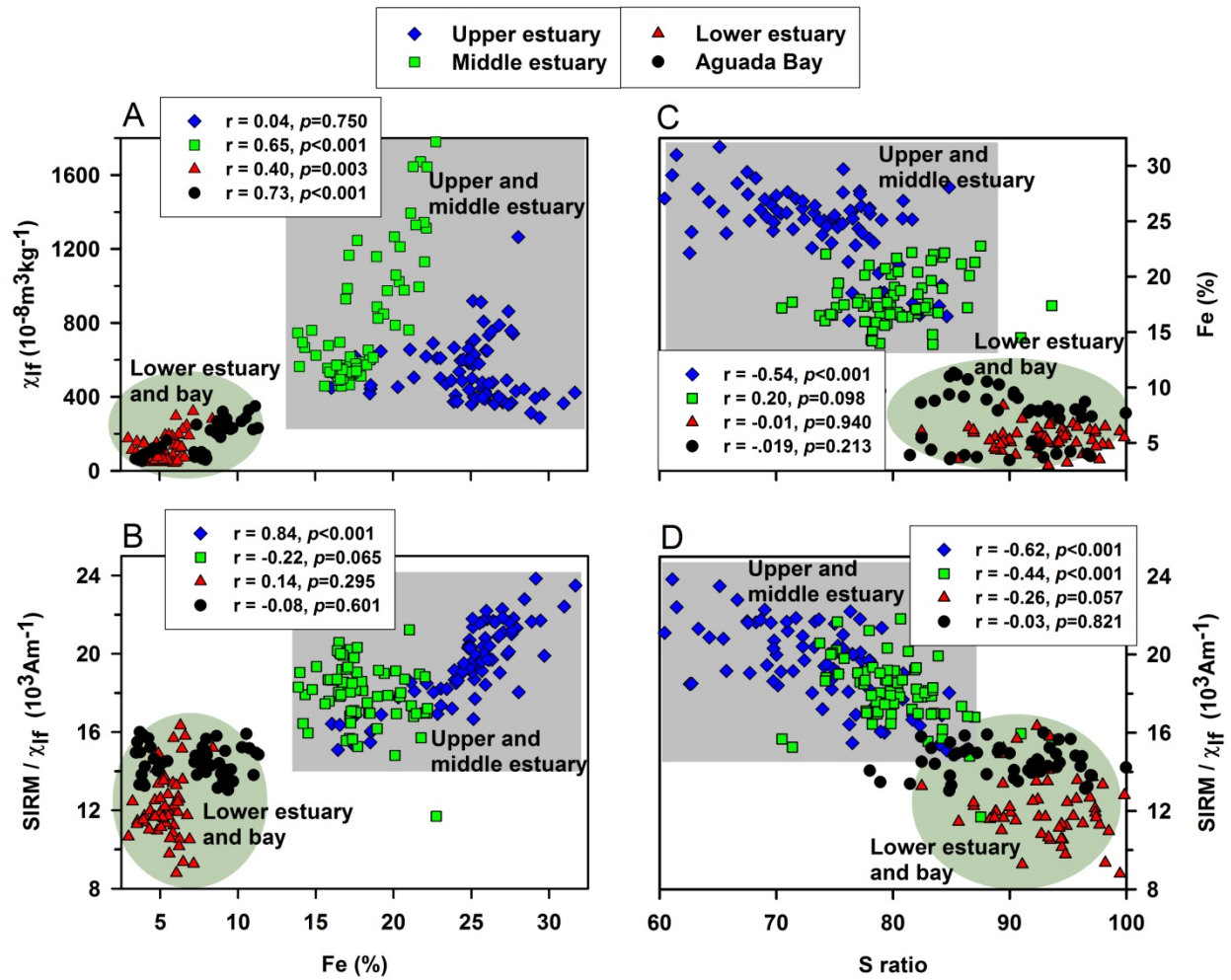


Figure 6

Lower estuary

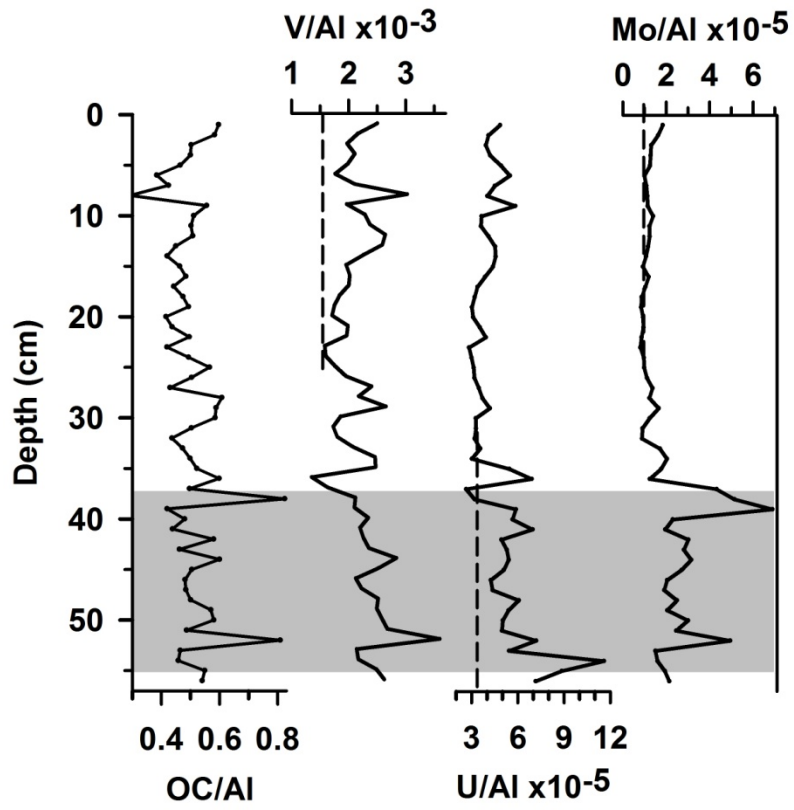


Figure 7

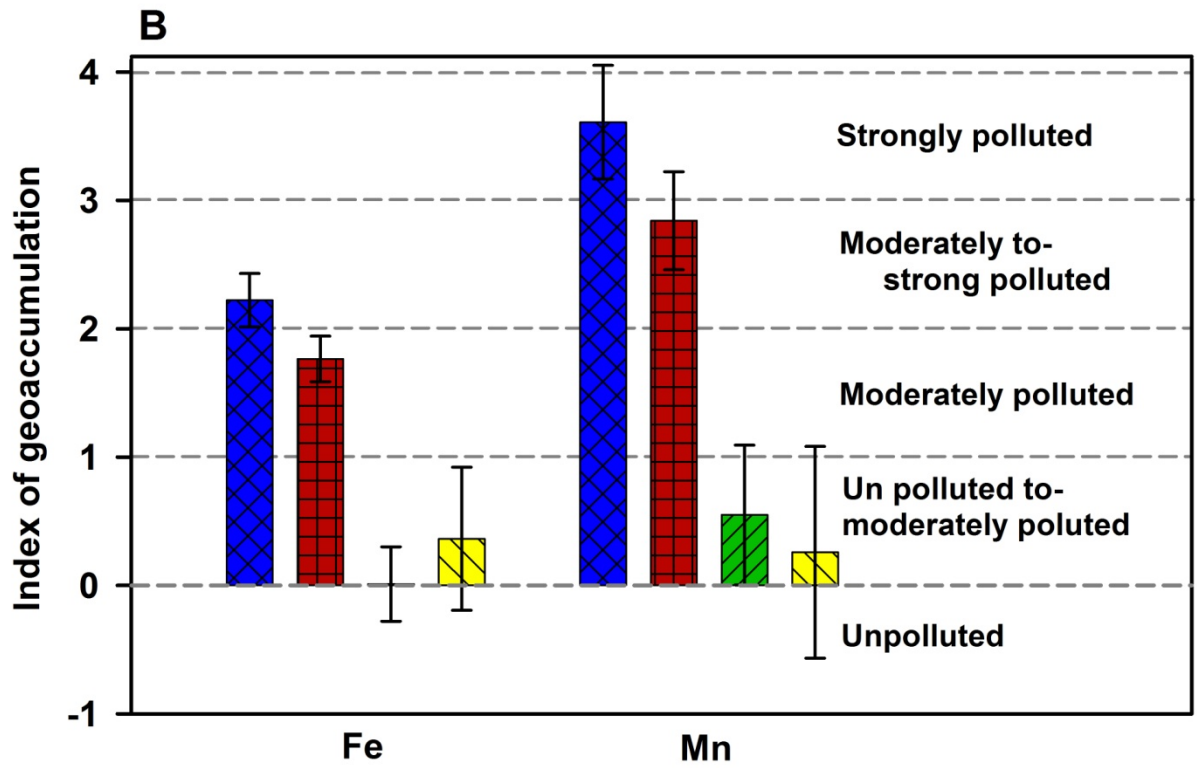
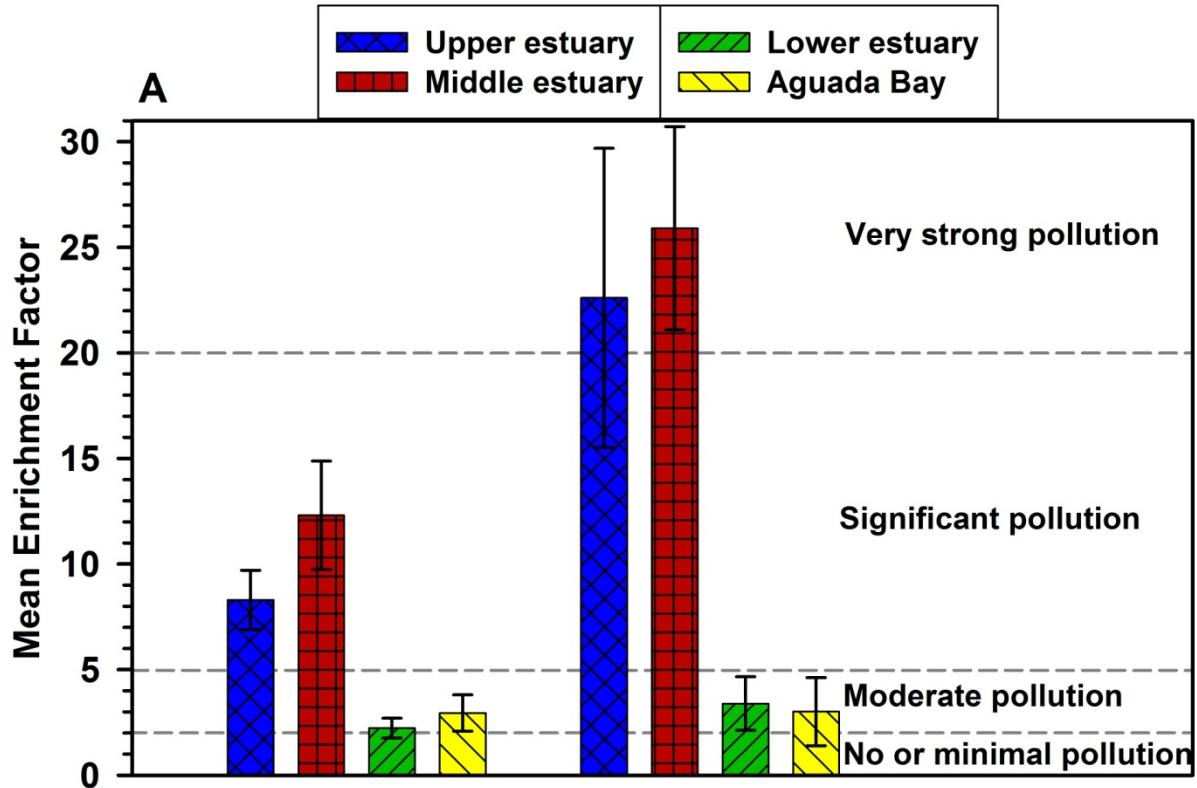


Figure 8

Table 1 Range and mean values of magnetic parameters, Fe and Mn concentrations in sediment cores from the Mandovi estuary.

		Upper estuary (3 cores)	Middle estuary (2 cores)	Lower estuary (1 core)	Aguada Bay (1 core)	Iron ore
Length of recovered sediment in cores		54 – 79 cm	72 – 79 cm	56 cm	47 cm	
χ_{if} ($10^{-8}m^3kg^{-1}$)	Min	229.5 - 287.1	360.1 - 458.1	41.3	52.9	2130
	Max	1188.1 - 2194.2	728.5 - 1779.2	322.3	349.7	
	Mean	617.0	655.6	121.7	154.7	
	SD	481.1	355.9	69.7	90.9	
χ_{ARM} ($10^{-5}m^3kg^{-1}$)	Min	1 - 1.3	1.4 - 1.5	0.1	0.2	5.6
	Max	2.2 - 2.5	2.1 - 3.2	2.3	1.2	
	Mean	1.6	1.9	0.9	0.6	
	SD	0.4	0.2	0.7	0.3	
SIRM ($10^{-3}Am^2Kg^{-1}$)	Min	28.1 - 77.1	64.2 - 79.8	5.0	7.1	929.6
	Max	225.0 - 349.2	147.9 - 282.8	42.5	52.3	
	Mean	123.2	116.9	14.5	22.4	
	SD	63.1	53.6	7.4	13.1	
$\chi_{fd}\%$	Min	0.1 - 0.4	0.1 - 0.2	0.1	0.1	2.4
	Max	5.9 - 6.8	7.3 - 6.7	11.0	7.6	
	Mean	2.7	3.1	4.5	2.5	
	SD	1.7	1.8	3.3	1.6	
χ_{ARM}/χ_{if}	Min	0.9 - 1.7	1.4 - 2.9	1.4	2.3	2.6
	Max	5.3 - 6.4	4.3 - 4.4	12.3	10.9	
	Mean	3.1	3.2	6.6	4.8	
	SD	1.0	0.8	3.1	2.5	
SIRM/ χ_{if}	Min	9.2 - 15.1	11.7 - 15.8	8.8	13.0	43.6
	Max	23.8 - 39.7	20.5 - 21.8	16.3	16.0	
	Mean	23.4	18.1	12.3	14.5	
	SD	7.9	1.7	1.7	0.8	
$\chi_{ARM}/SIRM$ ($10^{-5}mA^{-1}$)	Min	4.9 - 9.9	8.2 - 14.1	12.8	16.6	6.1
	Max	17.9 - 41.2	24.6 - 26.4	112.1	70.0	
	Mean	15.6	17.7	54.9	33.1	
	SD	5.5	2.7	27.7	16.5	
S-ratio (%)	Min	43.65 - 63.2	69.1 - 70.5	82.5	78.0	88.7
	Max	80.7 - 94.2	93.6 - 94.74	99.8	100.0	
	Mean	72.7	80.1	92.8	89.8	
	SD	8.1	4.4	3.8	5.3	
Fe (%)	Min	16.0	13.9	3.0	3.4	50.9
	Max	31.7	22.8	8.4	11.3	
	Mean	24.8 (5.05) [#]	18.0	5.4	7.2	
	SD	3.3	2.2	1.0	2.5	
Mn (%)	Min	0.54	0.31	0.05	0.04	1.2
	Max	1.98	0.99	0.29	0.30	
	Mean	1.15 (0.085) [#]	0.67	0.14	0.13	
	SD	0.33	0.16	0.05	0.07	

[#] The values in brackets are for the Post- Archean average Australian Shale (PAAS).